Sciencexpress Reports

Rapid Progression of Ocean Acidification in the California Current System

Nicolas Gruber,[1]* Claudine Hauri,[1] Zouhair Lachkar,[1] Damian Loher,[1] Thomas L. Frölicher,[2] Gian-Kasper Plattner[3]

[1]Environmental Physics, Institute of Biogeochemistry and Pollutant Dynamics, ETH Zurich, Zurich, Switzerland.

[2]AOS Program, Princeton University, Princeton, NJ, USA.

[3]Climate and Environmental Physics, University of Bern, Bern, Switzerland.

*To whom correspondence should be addressed. E-mail: nicolas.gruber@env.ethz.ch

Nearshore waters of the California Current System (California CS) already today have a low carbonate saturation state, making them particularly susceptible to ocean acidification. Here, we use eddy-resolving model simulations to study the potential development of ocean acidification in this system up to 2050 under the SRES A2 and B1 scenarios. In both scenarios, the saturation state of aragonite Ω_{arag} is projected to drop rapidly, with much of the nearshore regions developing summer-long undersaturation in the top 60 m within the next 30 years. By the year 2050, waters with Ω_{arag} above 1.5 have largely disappeared and more than half of the waters are undersaturated year-round. Habitats along the seafloor become exposed to year-round undersaturation within the next 20 to 30 years. This has potentially major implications for the rich and diverse ecosystem that characterizes the California CS.

While it has been known for decades that the oceanic uptake of anthropogenic CO_2 will lead to a reduction in the pH of seawater (*1*, *2*), these changes were considered to be of an amplitude too small to harm marine organisms or to lead to appreciable changes in the biogeochemical cycling of elements in the ocean. It was only when first experimental results revealed that certain marine organisms respond sensitively to this CO_2-induced reduction in pH or to the associated changes in marine carbonate chemistry—aka ocean acidification—that the scientific community began to realize that this is a potentially serious issue (*3*–*6*). The carbonate saturation state, Ω, is of particular relevance, especially for organisms that build part of their structures out of mineral forms of $CaCO_3$. Ω describes whether seawater is super- or undersaturated with regard to mineral forms of $CaCO_3$, such as calcite or the less stable forms aragonite and high magnesium carbonate (*7*). When $\Omega > 1$, seawater is supersaturated, while $\Omega < 1$ characterizes seawater that is undersaturated. Currently, nearly all of the surface ocean waters are substantially supersaturated with regard to aragonite (global mean Ω_{arag} of ~3.0) (*8*). However, upwelling regions such as the Southern Ocean (*9*, *10*) and the Eastern Boundary Upwelling Systems (*11*) have naturally a lower pH and a substantially lower saturation state. This is because the upwelled waters are enriched in CO_2 from the remineralization of organic matter in the ocean interior, and thus have low pH and Ω.

Recent observations in the California Current System (California CS), one of the four major Eastern Boundary Upwelling Systems, revealed that waters with $\Omega_{arag} < 1$ are being transported onto the continental shelf during strong upwelling events, and even reaching the surface ocean in a few nearshore locations (*11*). While the upwelling of waters with low pH and Ω_{arag} is a naturally occurring event along the U.S. West Coast (*12*, *13*), model and data-based estimates suggest that the increase in atmospheric CO_2 since pre-industrial times has contributed to the severity of the event, by lowering pH by ~0.1 and Ω_{arag} by ~0.4 (*11*, *12*). With atmospheric CO_2 likely to increase further, it is important to assess how the California CS will evolve in the future and what levels of ocean acidification it might experience in the coming decades. This is especially relevant since the California CS constitutes one of the most productive ecosystems in the world with a high biodiversity (*14*, *15*) and important commercial fisheries (*16*), yet may be particularly prone to reaching widespread undersaturation soon due to its low initial pH and Ω_{arag}. Global ocean models have failed so far to recognize ocean acidification in Eastern Boundary Upwelling Systems (*17*), since their coarse resolution is insufficient to resolve the local dynamics responsible for bringing the waters with low pH and Ω_{arag} to the surface (*9*, *18*, *19*). We overcome this limitation here by using a regional model at eddy-resolving resolution, and investigate the progression of ocean acidification in the California CS from 1995 until 2050 under two future CO_2 scenarios, i.e., the "high" emissions SRES scenario A2 and the "low" emissions SRES scenario B1 (*20*). We contrast these projections into the future with results from a simulation of the pre-industrial state, i.e., 1750. We put particular emphasis on the changes in the saturation state Ω_{arag} in the nearshore 10 km region of the central California CS [Point Conception (34°35′N) to the California/Oregon border (42°0′N)], where upwelling is strongest.

The model we employ is a California CS setup of the Regional Oceanic Modeling System (ROMS) (*21*), to which we have coupled a simple nitrogen-based ecosystem model and a full description of the marine inorganic carbon system (*22*, *23*) (see supplementary materials for details and model evaluation). For all simulations, the model is forced with present-day climatological boundary conditions based on observations, except for atmospheric CO_2 and for the lateral boundary conditions of dissolved inorganic carbon, *DIC*. For the pre-industrial time-slice simulation, atmospheric pCO_2 was prescribed at 280 ppm, while for the transient simulations, atmospheric pCO_2 increased from 364 ppm in 1995 to 492 ppm (B1 scenario) and 541 ppm (A2 scenario), respectively, in 2050. The pre-industrial case and the A2 scenario were run with our standard configuration at 5 km horizontal resolution, while we employed a coarser-resolution configuration of 15 km to explore the sensitivity of our results to the scenarios.

For the time period between 1750 and 2005, the model simulations suggest that surface ocean pH decreased from an annual mean for the whole California CS of 8.12 ± 0.03 to 8.04 ± 0.03 (1 standard deviation of the spatial mean) (Fig. 1). Over the same time period, the annual mean surface ocean Ω_{arag} decreased from 2.58 ± 0.19 to 2.27 ± 0.20 reflecting the reduction of the carbonate ion concentration from the titration of the CO_2 that the ocean has taken up from the atmosphere. In the nearshore 10 km of the central California Coast annual mean surface pH and Ω_{arag} in 1750 already were as low as 8.03 ± 0.03, and 1.94 ± 0.14, respectively, reflecting the upwelling of waters with naturally low pH and Ω_{arag} due to the substantial addition of respired CO_2 to these waters. The uptake of anthropogenic CO_2 from the atmosphere until 2005 de-

creased the surface pH and Ω_{arag} in this region by about the same amount as for the whole domain, yielding annual mean values of 7.95 ± 0.04 and 1.67 ± 0.16, respectively.

For atmospheric pCO_2 following the SRES-A2 scenario, our model simulation predicts an even sharper decrease until 2050 to an annual mean surface pH and Ω_{arag} for the whole domain of 7.92 ± 0.03 and 1.77 ± 0.16, and for the nearshore 10 km environment of the central California CS to 7.82 ± 0.04 and 1.26 ± 0.12, respectively. pH and Ω_{arag} reach even lower values in summer, when upwelling is at its maximum (*13*). In July, for example, our model projects for 2050 that large stretches of the nearshore 10 km of the central California CS will be undersaturated (supplementary materials), although the mean Ω_{arag} remains slightly supersaturated (1.05 ± 0.13).

These changes are not confined to the surface ocean, as anthropogenic CO_2 is transported from the surface to depth, causing changes in the carbonate chemistry there as well (Fig. 1, D to F). As a result, the aragonite saturation horizon, which was located at about 350 m in the offshore region, and at about 300 m in the nearshore, shoaled generally by about 150 m from 1750 until 2005, and is projected to shoal by another 100 to 150 m between 2005 and 2050. In 2050, the annual mean aragonite saturation horizon is as shallow as 100 m in the offshore region, but shoals to less than 50 m in the nearshore regions in the annual mean. In the summer, the aragonite saturation horizon breaks to the surface in many parts of the central California CS (fig. S4). Thus, ocean acidification will severely reduce the habitat for organisms that are sensitive to the saturation state, and particularly for those who cannot tolerate undersaturated conditions for an extensive period of time.

The reduction of habitats of organisms sensitive to ocean acidification becomes even more evident when considering the volume of water with a particular range of saturation states within the nearshore 10 km of the central California CS (cf. Fig. 2). In 1750, our model simulates that about 16% of the waters in the euphotic zone (0 to 60 m) in that region had an Ω_{arag} above 2 with the majority (60%) having an Ω_{arag} between 1.5 and 2.0 (Fig. 2A). Only 24% of the waters had an Ω_{arag} between 1.5 and 1.0, and no waters were undersaturated. By 2005, the volume of waters with an Ω_{arag} greater than 1.5 had dropped to about 20% in the yearly average, with waters with an Ω_{arag} between 1.0 and 1.5 dominating, and undersaturated waters appearing seasonally. In the coming decades, waters with an Ω_{arag} less than 1 are projected to expand substantially in the euphotic zone of the central California CS, occupying more than half of the waters in 2050 in the annual mean. In the summer season, this ratio increases to about 70%, with long stretches of the central coast projected to be undersaturated throughout the euphotic zone (fig. S4). By that time, waters with an Ω_{arag} above 1.5 will have largely vanished.

The progression toward wide-spread and persistent undersaturation in the nearshore 10 km is even more dramatic in the upper twilight zone, i.e., in the depth range between 60 and 120 m (Fig. 2B). While nearly all waters in this depth range were supersaturated with respect to aragonite in pre-industrial times, a small, but persistent volume of undersaturated waters appears by 2005. Within the next 20 to 30 years, the volume of undersaturated waters quickly expands, and by around 2035 in the SRES A2 scenario, nearly the entire twilight zone of the central California Coast will be undersaturated year-round.

In the bottom layer of the model above the shelf sediments of the central California CS (with water depths ranging between 50 and maximally 120 m) undersaturated conditions had become common by 2005 (Fig. 2C). This is a substantial change since pre-industrial times, where the model simulated no undersaturated conditions in this layer. Yet, still about 30% of this layer remains supersaturated in 2005. Our simulations for the waters above the shelf sediments are consistent with data-based reconstructions for the central Oregon coast (*13*), which also suggest widespread undersaturated conditions for the present, but also extended periods of supersaturation with regard to aragonite. Such supersaturated conditions are projected to disappear within the next 10 years, so that by the mid-2020s, essentially all waters above the shelf sediments will be undersaturated.

Most of these early developments occur irrespective of whether atmospheric CO_2 follows the "high" (A2) or the "low" (B1) CO_2 scenario (see supplementary materials). This lack of sensitivity is due to two factors. First, the two scenarios do not differ substantially in their atmospheric CO_2 levels for the next 20 years, and only around 2035 begin to deviate more strongly from each other (fig. S5). Second, since surface waters are following the increase in atmospheric CO_2 relatively closely, the primary determinant for the degree of ocean acidification in the upper ocean is the atmospheric CO_2 concentration and not its rate of change. This is well illustrated when the saturation state is plotted as a function of atmospheric pCO_2 rather than time (Fig. 3), resulting in nearly identical results for the two scenarios (fig. S7). This means that the timing of when particular chemical thresholds are reached in the upper ocean depends only on when the corresponding atmospheric CO_2 concentration is attained. Our simulation results show that at ~400 ppm substantial parts of the twilight zone (60 to 120 m) and the habitats along the seafloor on the shelf become undersaturated. Given the present day atmospheric CO_2 concentration of 390 ppm and the recent rates of increase in atmospheric CO_2 of 1.5 ppm/year or more (*24*), a level of 400 ppm is virtually certain to be reached within this decade. When atmospheric CO_2 reaches ~500 ppm, the top 60 m in our model begin to experience extended undersaturated conditions, a level which is crossed by ~2040 in the A2 scenario, and a little after 2050 in the B1 scenario. Thus, unless atmospheric CO_2 follows a scenario that is much lower than the "low emission" B1 pathway, most of the simulated transitions are bound to happen.

The projected evolution of the upper ocean in the nearshore 10 km of the central California CS toward low Ω_{arag} conditions is similar to that projected for the Southern Ocean and the Arctic (Fig. 3), which previously have been proposed as the first oceanic regions to become undersaturated (*9*, *18*). The upper twilight zone and the bottom layer of the central California CS become undersaturated even faster than the surface Arctic, highlighting the imminent nature of reaching this threshold.

The progression of ocean acidification may occur even faster or at lower atmospheric CO_2 concentrations than projected by our model simulations. First, our model tends to overpredict Ω_{arag} in the nearshore regions (see supplementary materials), so that the appearance of certain Ω_{arag} thresholds is likely delayed in the model. A sensitivity test, where we applied a uniform correction of –0.1 units to Ω_{arag} reveals that the shifts in the distribution of volumina with a particular saturation state may occur about 10 years earlier than in our standard case (see fig. S3). Second, our model is forced with the present-day climatological boundary conditions for all years up to 2050, while theoretical considerations (*25*), model simulations (*26*), and historical trends (*27*) suggest that the upwelling favorable winds may increase in the coming decades in response to global warming. This could enhance the upwelling of corrosive water and accelerate the progression toward low Ω_{arag} conditions even further.

While we are able to project the chemical changes associated with the future evolution of ocean acidification in the California Current System with some confidence, the impacts of these chemical changes on organisms, ecosystems and biogeochemistry remain highly uncertain (*6*, *28*, *29*). The limited evidence available suggests that most aragonite secreting organisms, such as pteropods or oysters respond negatively to lowered Ω_{arag} (*30*), with the early life stages appearing to be particularly sensitive (*31*). We emphasize here the progression toward undersaturated conditions, as this represents a well established chemical threshold, but note that none of the organisms studied so far has a simple dose response

curve with a threshold at $\Omega_{arag} = 1$ (*28*). Rather, some organisms or life stages respond already negatively at higher Ω_{arag}, while others can tolerate undersaturated conditions for some time. In addition, organisms living in the California CS might have had the chance to adapt to the naturally low and variable pH and Ω_{arag} conditions that prevailed already before the onset of the industrial revolution, making them potentially less vulnerable to the effects of ocean acidification (*32*). Regardless of these uncertainties associated with the biological response to ocean acidification, our simulation results indicate that the California CS is moving rapidly toward conditions that are well outside the natural range with frequent or even persistent undersaturation conditions (cf. Fig. 3). Such conditions likely will be challenging to calcifying and other organisms and the fisheries that depend on them (*33*).

Although we focused in this study here on the changes in Ω_{arag}, ocean acidification alters all aspects of the carbonate chemistry in the ocean, including pH and the concentrations of dissolved CO_2, bicarbonate, and carbonate (*34*), each of which can impact physiological processes and hence affect marine organisms and ecosystems (*35*). The changes in these properties are highly correlated (fig. S7), though, since they are mechanistically linked through the driver of OA, i.e., the oceanic uptake of CO_2 from the atmosphere. This increases dissolved CO_2 and bicarbonate, but decreases pH, Ω_{arag}, and carbonate with predictable ratios (*34*). Therefore, regardless of whether the parameter impacting a biological process is Ω_{arag} or the dissolved CO_2 concentration, the changes are unprecedented.

In addition, ocean acidification will not be operating in isolation, but its impact could be potentially worsened with synergistic effects of ocean warming and ocean deoxygenation (*35*, *36*), both of which are also observed to occur in the California CS (*37*, *38*) and likely get more severe as well (*39*). Thus, specific attention should be given to the development of ocean acidification in this very rich and productive ecosystem, and also to some of the other Eastern Boundary Current Systems where similar conditions prevail.

References and Notes

1. W. Stumm, J. J. Morgan, Aquatic Chemistry: An Introduction Emphasizing Chemical Equilibria in Natural Waters (Wiley Interscience, New York, ed. 1, 1970).
2. W. S. Broecker, Y.-H. Li, T.-H. Peng, *Impingement of Man on the Oceans*, D. W. Hood, Ed. (Wiley, New York, 1971), pp. 287–324.
3. J.-P. Gattuso, M. Frankignoulle, I. Bourge, S. Romaine, R. W. Buddemeier, Effect of calcium carbonate saturation of seawater on coral calcification. *Global Planet. Change* **18**, 37 (1998). doi:10.1016/S0921-8181(98)00035-6
4. J. A. Kleypas *et al*., Geochemical consequences of increased atmospheric carbon dioxide on coral reefs. *Science* **284**, 118 (1999). doi:10.1126/science.284.5411.118 Medline
5. U. Riebesell *et al*., Reduced calcification of marine plankton in response to increased atmospheric CO_2. *Nature* **407**, 364 (2000). doi:10.1038/35030078 Medline
6. S. C. Doney, V. J. Fabry, R. A. Feely, J. A. Kleypas, Ocean acidification: The other CO_2 problem. *Annu. Rev. Mar. Sci.* **1**, 169 (2009). doi:10.1146/annurev.marine.010908.163834
7. A. Mucci, The solubility of calcite and aragonite in seawater at various salinities, temperatures, and one atmosphere total pressure. *Am. J. Sci.* **283**, 781 (1983). doi:10.2475/ajs.283.7.780
8. R. A. Feely, S. C. Doney, S. C. Cooley, Ocean acidification: Present conditions and future changes in a high-CO_2 world. *Oceanography* **22**, 36 (2009). doi:10.5670/oceanog.2009.95
9. J. C. Orr *et al*., Anthropogenic ocean acidification over the twenty-first century and its impact on calcifying organisms. *Nature* **437**, 681 (2005). doi:10.1038/nature04095 Medline
10. B. I. McNeil, R. J. Matear, Southern Ocean acidification: A tipping point at 450-ppm atmospheric CO_2. *Proc. Natl. Acad. Sci. U.S.A.* **105**, 18860 (2008). doi:10.1073/pnas.0806318105 Medline
11. R. A. Feely, C. L. Sabine, J. M. Hernandez-Ayon, D. Ianson, B. Hales, Evidence for upwelling of corrosive "acidified" water onto the continental shelf. *Science* **320**, 1490 (2008). doi:10.1126/science.1155676 Medline
12. C. Hauri *et al*., Ocean acidification in the California Current System. *Oceanography* **22**, 60 (2009). doi:10.5670/oceanog.2009.97
13. L. W. Juranek *et al*., A novel method for determination of aragonite saturation state on the continental shelf of central Oregon using multi-parameter relationships with hydrographic data. *Geophys. Res. Lett.* **36**, L24601 (2009). doi:10.1029/2009GL040778
14. M.-E. Carr, Estimation of potential productivity in Eastern Boundary Currents using remote sensing. *Deep Sea Res. Part II* **49**, 59 (2002). doi:10.1016/S0967-0645(01)00094-7
15. B. A. Block *et al*., Tracking apex marine predator movements in a dynamic ocean. *Nature* **415**, 86 (2011). doi:10.1038/nature10082
16. R. Costanza *et al*., The value of the world's ecosystem services and natural capital. *Nature* **387**, 253 (1997). doi:10.1038/387253a0
17. C. Turley *et al*., The societal challenge of ocean acidification. *Mar. Pollut. Bull.* **60**, 787 (2010). doi:10.1016/j.marpolbul.2010.05.006 Medline
18. M. Steinacher, F. Joos, T. L. Frölicher, G.-K. Plattner, S. C. Doney, Imminent ocean acidification in the Arctic projected with the NCAR global coupled carbon cycle-climate model. *Biogeosciences* **6**, 515 (2009). doi:10.5194/bg-6-515-2009
19. F. Joos, T. L. Frölicher, M. Steinacher, G.-K. Plattner, in *Ocean Acidification*, J.-P. Gattuso, L. Hansson, Eds. (Oxford Univ. Press, Oxford, 2011), chap. 14, pp. 272–290.
20. N. Nakicenovic et al., Special Report on Emissions Scenarios: A Special Report of Working Group III of the Intergovernmental Panel on Climate Change (Cambridge Univ. Press, New York, 2000).
21. A. F. Shchepetkin, J. C. McWilliams, The regional oceanic modeling system (ROMS): A split-explicit, free-surface, topography-following-coordinate oceanic model. *Ocean Model.* **9**, 347 (2005). doi:10.1016/j.ocemod.2004.08.002
22. N. Gruber *et al*., Eddy-induced reduction of biological production in eastern boundary upwelling systems. *Nat. Geosci.* **4**, 787 (2011).
23. Z. Lachkar, N. Gruber, What controls biological production in coastal upwelling systems? Insights from a comparative modeling study. *Biogeosciences* **8**, 2961 (2011). doi:10.5194/bg-8-2961-2011
24. P. Tans, R. F. Keeling, Recent Mauna Loa Data, *Electronic Data*, NOAA ESRL, Scripps Institution of Oceanography, Boulder, CO, USA (2012). www.esrl.noaa.gov/gmd/ccgg/trends/.
25. A. Bakun, Global climate change and intensification of coastal ocean upwelling. *Science* **247**, 198 (1990). doi:10.1126/science.247.4939.198 Medline
26. N. S. Diffenbaugh, M. A. Snyder, L. C. Sloan, Could CO_2-induced land-cover feedbacks alter near-shore upwelling regimes? *Proc. Natl. Acad. Sci. U.S.A.* **101**, 27 (2004). doi:10.1073/pnas.0305746101 Medline
27. D. Gutiérrez *et al*., Coastal cooling and increased productivity in the main upwelling zone off Peru since the mid-twentieth century. *Geophys. Res. Lett.* **38**, L07603 (2011). doi:10.1029/2010GL046324
28. K. J. Kroeker, R. L. Kordas, R. N. Crim, G. G. Singh, Meta-analysis reveals negative yet variable effects of ocean acidification on marine organisms. *Ecol. Lett.* **13**, 1419 (2010). doi:10.1111/j.1461-0248.2010.01518.x Medline
29. J. P. Barry, S. Widdicombe, J. M. Hall-Spencer, in *Ocean Acidification*, J.-P. Gattuso, L. Hansson, Eds. (Oxford Univ. Press, Oxford, 2011), chap. 10, pp. 192–209.
30. V. J. Fabry, B. A. Seibel, R. A. Feely, J. C. Orr, Impacts of ocean acidification on marine fauna and ecosystem processes. *ICES J. Mar. Sci.* **65**, 414 (2008). doi:10.1093/icesjms/fsn048
31. A. Barton, B. Hales, G. G. Waldbusser, C. Langdon, R. Feely, The Pacific oyster, *Crassostrea gigas*, shows negative correlation to naturally elevated carbon dioxide levels: Implications for near-term ocean acidification effects. *Limnol. Oceanogr.* **57**, 698 (2012). doi:10.4319/lo.2012.57.3.0698
32. M. D. Ohman, B. E. Lavaniegos, A. W. Townsend, Multi-decadal variations in calcareous holozooplankton in the California Current System: Thecosome pteropods, heteropods, and foraminifera. *Geophys. Res. Lett.* **36**, L18608 (2009). doi:10.1029/2009GL039901
33. S. R. Cooley, S. C. Doney, Anticipating ocean acidification's economic consequences for commercial fisheries. *Environ. Res. Lett.* **4**, 024007 (2009). doi:10.1088/1748-9326/4/2/024007
34. J. C. Orr, in *Ocean Acidification*, J. P. Gattuso, L. Hansson, Eds. (Oxford Univ. Press, 2011), chap. 3, pp. 41–66.

35. H. O. Pörtner, Ecosystem effects of ocean acidification in times of ocean warming: A physiologist's view. *Mar. Ecol. Prog. Ser.* **373**, 203 (2008). doi:10.3354/meps07768
36. N. Gruber, Warming up, turning sour, losing breath: Ocean biogeochemistry under global change. *Philos. Trans. R. Soc. London Ser. A* **369**, 1980 (2011).
37. S. J. Bograd *et al*., Oxygen declines and the shoaling of the hypoxic boundary in the California Current. *Geophys. Res. Lett.* **35**, L12607 (2008). doi:10.1029/2008GL034185
38. F. Chan *et al*., Emergence of anoxia in the California current large marine ecosystem. *Science* **319**, 920 (2008). doi:10.1126/science.1149016 Medline
39. R. F. Keeling, A. Kortzinger, N. Gruber, Ocean deoxygenation in a warming world. *Annu. Rev. Mar. Sci.* **2**, 199 (2010). doi:10.1146/annurev.marine.010908.163855

Acknowledgments: This work was supported by ETH Zürich and the European Project on Ocean Acidification (EPOCA), which received funding from the European Community's Seventh Framework Programme (FP7/2007-2013) under grant agreement no. 211384. T.L.F. was supported by the Carbon Mitigation Initiative project at Princeton Univ., sponsored by BP and Ford Motor Company. We thank J. C. McWilliams and his group at UCLA for the long-term collaboration on the development of ROMS.

Supplementary Materials
www.sciencemag.org/cgi/content/full/science.1216773/DC1
Supplementary Text
Figs. S1 to S8
References

17 November 2011; accepted 30 May 2012
Published online 14 June 2012
10.1126/science.1216773

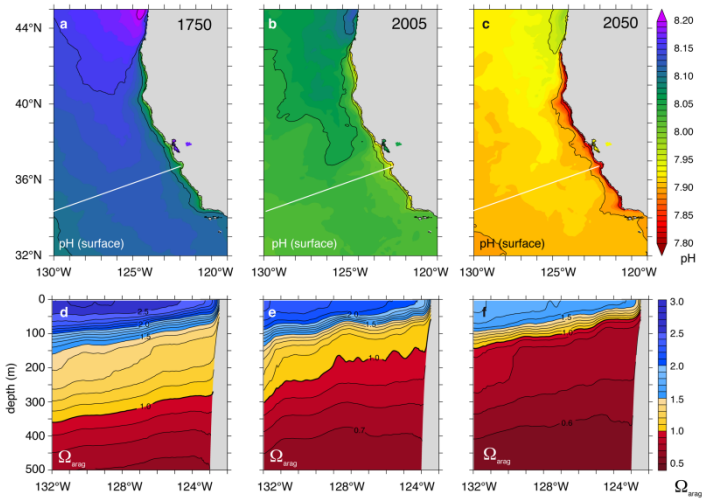

Fig. 1. Temporal evolution of ocean acidification in the California Current System from 1750 until 2050 for the A2 scenario. (**A** to **C**) Maps illustrating the evolution of annual mean surface pH, illustrating the decrease in pH for the three time slots 1750, 2005, and 2050. (**D** to **F**) Offshore depth sections depicting the general decrease of the annual mean saturation state of seawater with regard to aragonite, Ω_{arag}, and the shoaling of the saturation depth, i.e., Ω_{arag} = 1, for the same three time slots. The white lines in (A) to (C) indicate the position of the offshore section.

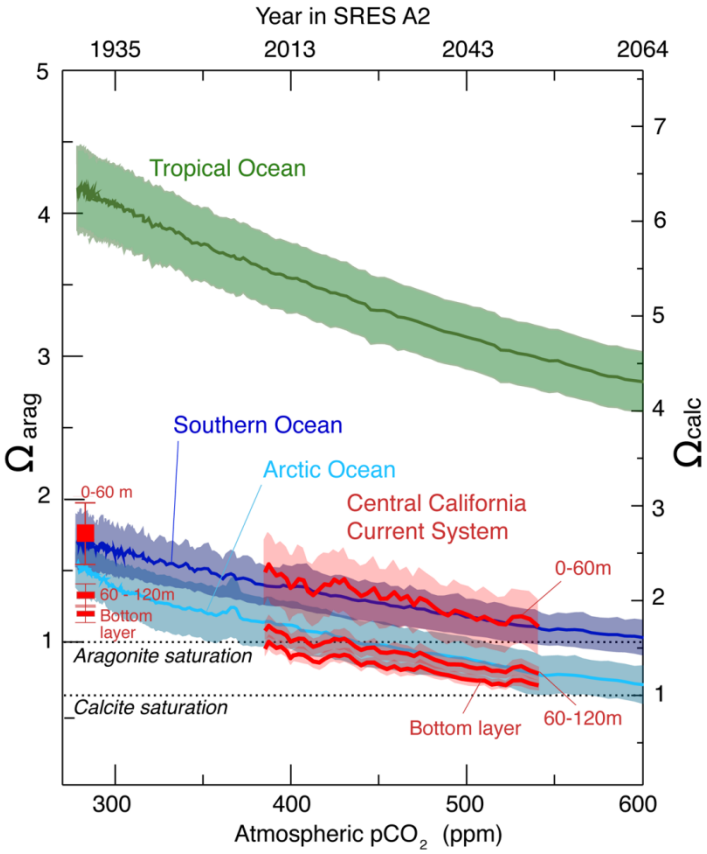

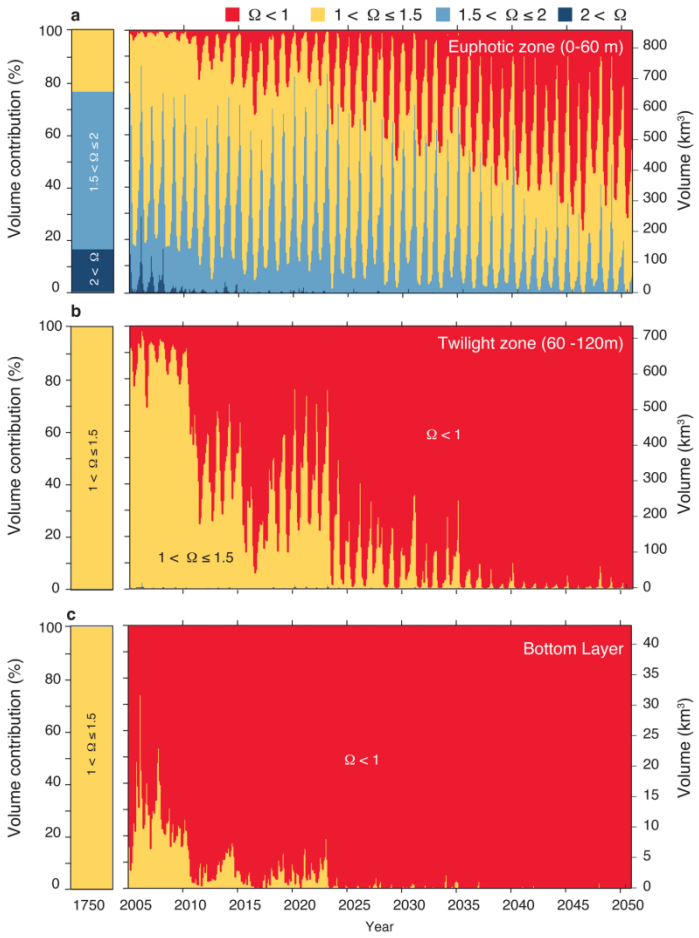

Fig. 2. Temporal evolution of the volume of seawater with a particular aragonite saturation state, Ω_{arag} in the nearshore 10 km of the central California CS for the A2 scenario. The panels depict the evolution (**A**) in the upper 60 m, (**B**) in between 60 and 120 m, and (**C**) in the bottom layer of the model above the shelf sediments (maximum depth 120 m). The volumes were computed by summing over all regions from Point Conception (34°35′N) to the California/Oregon border (42°0′N).

Fig. 3. Temporal evolution of the mean saturation states with regard to aragonite (left *y* axis) and calcite (right *y* axis) in the nearshore 10 km of the central California Current System as a function of the atmospheric partial pressure of CO_2, i.e., pCO_2 (lower *x* axis), and time (upper *x* axis). Depicted are the evolution of three depth layers, i.e., 0 to 60 m, 60 to 120 m, and the bottom layer of the model above the shelf sediments. Also shown are the mean evolutions of Ω_{arag} for the tropical ocean, for the Southern Ocean, and for the Arctic as simulated by a global coarse resolution model (*18*). Shaded curves depict the modeled trajectories including ±1 standard deviation of the seasonal variations. All simulations are done for the A2 scenario.